J|A|C|S
ARTICLES
Published on Web 09/21/2004

A Sequential Molecular Mechanics/Quantum Mechanics Study of the Electronic Spectra of Amides

Nicholas A. Besley,* Mark T. Oakley, Alexander J. Cowan, and Jonathan D. Hirst

Contribution from the School of Chemistry, University of Nottingham, University Park, Nottingham, NG7 2RD, U.K.

Received April 26, 2004; E-mail: nick.besley@nottingham.ac.uk

Abstract: We report gas-phase electronic spectra of formamide, *N*-methyformamide, acetamide, and *N*-methylacetamide at 300 K calculated using a combination of classical molecular dynamics and time-dependent density functional theory (TDDFT). In comparison to excitation energies computed using the global minima structures, the valence $n\pi^*$ and $\pi_{nb}\pi^*$ states show a significant red-shift of 0.1−0.35 eV, while smaller shifts are found for the n3s and π_{nb}3s Rydberg states. In this work, we have identified the physical origin of these shifts arising from variations of the molecular structure. We present simple relationships between key geometrical parameters and spectral shifts. Consequently, electronic spectra can be generated directly from ground-state structures, without additional quantum chemical calculations. The electronic spectrum of formamide in aqueous solution is computed using TDDFT using an explicit solvent model. This provides a quantitative determination of the condensed-phase spectrum. In general, this study shows that temperature effects can change the predicted excitation energies significantly and demonstrates how electronic spectra at elevated temperatures can be computed in a computationally efficient way.

Introduction

The vast majority of calculations of electronic excited states generally consider vertical excitations from the optimum ground-state geometry of the system. Consequently, an electronic transition is represented by a single energy and oscillator strength. However, molecular electronic transitions have a range of energies leading to a spectral band. This broadening can arise from thermal or electronic effects. The relative contribution of thermal and electronic effects to broadening in the density of states in liquid water has been examined.[1] If electronic spectra are to be simulated, then these effects need to be taken into account. To describe broadening arising from excitation to different vibrational states requires calculation of Franck−Condon factors, while to simulate thermal broadening requires consideration of the many structures that a molecule will adopt. Furthermore, the study of thermal broadening can provide insight into the relationship between spectral features and the underlying molecular structure. Solvent can also have a significant effect on electronic spectra, inducing changes in the position, intensity, and shape of spectral bands.[2] The calculation of electronic spectra in solution represents a significant challenge due to the size and complexity of the system. This study is concerned with the calculation of electronic spectra of amides in gas phase and aqueous solution at room temperature and the structural origin of the thermal broadening of the spectral bands.

The electronic structure of amides has been the focus of considerable interest for many years. These studies are motivated by the role of amides as a model for the fundamental repeating unit in the backbone of proteins. A variety of properties has been studied, for example, minimum energy structures, hydrogen bond strengths, and infrared spectroscopy.[3−13] These studies usually focus on the electronic ground state. In recent years, the development of time-resolved protein circular dichroism spectroscopy on the microsecond[14] and nanosecond[15] time scales has led to renewed interest in the electronic excited states of proteins. Currently, the excited states of proteins cannot be studied directly using quantitative quantum chemical methods.

(1) Hunt, P.; Sprik, M.; Vuilleumier, R. *Chem. Phys. Lett.* **2003**, *376*, 68−74.
(2) Suppan, P.; Ghoneim, N. *Solvatochromism*; The Royal Society of Chemistry: Cambridge, U.K., 1997.
(3) McCreery, J. H.; Christoffersen, R. E.; Hall, G. G. *J. Am. Chem. Soc.* **1976**, *98*, 7198−7202.
(4) Marchese, F. T.; Mehrotra, P. K.; Beveridge, D. L. *J. Phys. Chem.* **1984**, *88*, 5692−5702.
(5) Jorgensen, W. L.; Swenson, C. J. *J. Am. Chem. Soc.* **1985**, *107*, 1489−1496.
(6) Sneddon, S. F.; Tobias, D. J.; Brooks, C. L., III. *J. Mol. Biol.* **1989**, *209*, 817−820.
(7) Sim, F.; St-Amant, A.; Papai, I.; Salahub, D. R. *J. Am. Chem. Soc.* **1992**, *114*, 4391−4400.
(8) Contador, J. C.; Sanchez, M. L.; Aguilar, M. A.; Olivares del Valle, F. J. *J. Chem. Phys.* **1996**, *104*, 5539−5546.
(9) Adalsteinsson, H.; Maulitz, A. H.; Bruice, T. *J. Am. Chem. Soc.* **1996**, *118*, 7689−7693.
(10) Torii, H.; Tatsumi, T.; Kanazawa, T.; Tasumi, M. *J. Phys. Chem. B* **1998**, *102*, 309−314.
(11) Kubelka, J.; Keiderling, T. A. *J. Phys. Chem. A* **2001**, *105*, 10922−10928.
(12) Herrebout, W. A.; Clou, K.; Desseyn, H. O. *J. Phys. Chem. A* **2001**, *105*, 4865−4881.
(13) Watson, T. M.; Hirst, J. D. *J. Phys. Chem. A* **2002**, *106*, 7858−7867.
(14) Chen, E. F.; Wittung-Stafshede, P.; Kliger, D. S. *J. Am. Chem. Soc.* **1999**, *121*, 3811−3817.
(15) Zhang, C.-F.; Lewis, J. W.; Cerpa, R.; Kuntz, I. D.; Kliger, D. S. *J. Phys. Chem.* **1993**, *97*, 5499−5505.

10.1021/ja047603l CCC: $27.50

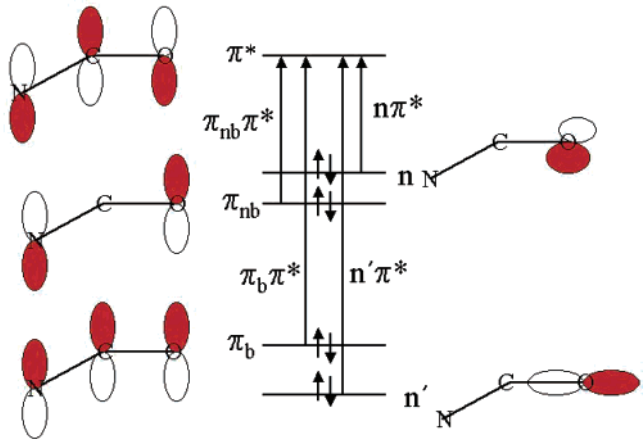

Figure 1. Valence molecular orbitals and electronic transitions of amides.

However, calculations of the excited states of amides provide an important step toward the calculation and interpretation of the excited states of proteins. In particular, parameters derived from calculations of amide excited states have contributed to accurate calculations of protein circular dichroism spectra.[16]

In gas phase, the electronic spectra of amides have been well-characterized (see Figure 1).[17−24] The spectra have an intense band, often labeled V_1, that corresponds to the $\pi_{nb}\pi^*$ (non-bonding π orbital to antibonding π^* orbital) transition. This transition occurs in the range 6.2−7.4 eV. The addition of alkyl groups to the amide nitrogen atom considerably decreases the $\pi_{nb}\pi^*$ excitation energy.[25] The nπ^* (lone pair on oxygen to π^* orbital) transition is termed the W band. This transition is much weaker and consequently more difficult to detect. However, it occurs typically in the region 5.5−5.8 eV.[23,24] In addition, there are sharp bands that correspond to transitions to Rydberg states. In formamide, a further band at higher energy (∼9 eV) called the Q-band was identified. The Q-band was originally assigned to the $\pi_b\pi^*$ transition, but more recently it has been shown to arise from a superposition of Rydberg states[26] while the $\pi_b\pi^*$ (bonding π orbital to antibonding π^* orbital) transition energy is greater than 10 eV.[24,27] At higher energy is a further transition corresponding to excitation from the second oxygen lone pair to the π^* orbital, denoted n′π^*.

Many theoretical investigations of electronic spectra of amides in gas phase have been reported.[20,24,26−34] These include multireference configuration interaction (MRCI) and complete active space self-consistent field method with multireference perturbation theory (CASSCF/CASPT2) calculations.[24,27,32] These calculations reproduce the excitation energies accurately and allow the spectral bands to the assigned. These studies also show that attaching an alkyl group to the amide nitrogen atom strongly decreases the $\pi_{nb}\pi^*$ transition energy and highlights problems associated with Rydberg valence mixing. Such calculations are appropriate for the system at 0 K. Simulation of electronic spectra at higher temperatures can be achieved through a combination of molecular dynamics simulation and quantum chemical calculations. Doltsinis and Sprik calculated the electronic spectrum of formamide at room temperature using a combination of ab initio molecular dynamics and time-dependent density functional theory (TDDFT), reproducing important spectral features.[26]

Solvent induces a number of changes in the spectra. The $\pi_{nb}\pi^*$ transition undergoes a red-shift. The magnitude of this shift varies for different amides and is dependent on the solvent. Experimental data indicate a red-shift of 0.40−0.5 eV for formamide[21] and a smaller red-shift of ∼0.1 eV for *N*-methylacetamide (NMA).[25,35] The origin of the red-shift is considered largely electrostatic in nature. In formamide, the permanent dipole moment of the $\pi_{nb}\pi^*$ state is 6.1 D compared with 4.1 D in the ground state.[24] Thus, the $\pi_{nb}\pi^*$ state has a more favorable interaction with a polar solvent.[25,36,37] Accurate determination of the effect of solvent on the nπ^* transition is difficult. In aqueous solution, a blue-shift of approximately 0.2−0.4 eV is observed.[25] This blue-shift arises as a result of hydrogen bonding between the amide and solvent. The ground state forms stronger hydrogen bonds than the excited nπ^* state, resulting in a blue-shift in the spectral band. However, the blue-shift observed in carbonyl nπ^* transitions has also been attributed to changes induced by hydrogen bonding in the geometry of the solute molecule.[38] This shift is not found in non-hydrogen bonding solvents.[21] Furthermore, in condensed phase the Rydberg bands are no longer observed.

Several groups have reported calculations of amide excited states in solution using solvent models of varying sophistication. These include calculations that incorporate a small number of solvent molecules, usually water, explicitly within the ab initio calculation.[39−41] Using a continuum solvent model, the electronic spectra of formamide and NMA were studied at the complete active space self-consistent field reaction field (CASSCF/SCRF) with CASPT2-RF level.[37] Generally, this approach adequately describes electrostatic effects. A red-shift was observed for the $\pi_{nb}\pi^*$ transition energies, but no significant blue-shift was found for the nπ^* transition. This work was later extended[42,43] to a combination of explicitly defined solvent and continuum description, in a so-called semicontinuum approach. By using this approach, both long and short range effects can be captured, and good agreement with the available experimental data was

(16) Besley, N. A.; Hirst, J. D. *J. Am. Chem. Soc.* **1999**, *121*, 9636−9644.
(17) Hunt, H. D.; Simpson, W. T. *J. Am. Chem. Soc.* **1953**, *75*, 4540−4543.
(18) Peterson, D. L.; Simpson, W. T. *J. Am. Chem. Soc.* **1957**, *79*, 2375−2382.
(19) Kaya, K.; Nagakura, S. *Theor. Chim. Acta* **1967**, *117*, 117−123.
(20) Basch, H.; Robin, M. B.; Kuebler, N. A. *J. Chem. Phys.* **1967**, *47*, 1201−1210.
(21) Basch, H.; Robin, M. B.; Kuebler, N. A. *J. Chem. Phys.* **1968**, *49*, 5007−5018.
(22) Staley, R. H.; Harding, L. B.; Goddard, W. A., III; Beauchamp, J. L. *Chem. Phys. Lett.* **1975**, *36*, 589−593.
(23) Gingell, J. M.; Mason, N. J.; Zhao, H.; Walker, I. C.; Siggel, M. R. F. *Chem. Phys.* **1997**, *220*, 191−205.
(24) Serrano-Andrés, L.; Fülscher, M. P. *J. Am. Chem. Soc.* **1996**, *118*, 12190−12199.
(25) Nielsen, E. B.; Schellman, J. A. *J. Phys. Chem.* **1967**, *71*, 2297−2304.
(26) Doltsinis, N. L.; Sprik, M. *Chem. Phys. Lett.* **2000**, *330*, 563−569.
(27) Hirst, J. D.; Hirst, D. M.; Brooks, C. L., III. *J. Phys. Chem.* **1996**, *100*, 13487−13491.
(28) Harding, L. B.; Goddard, W. A., III. *J. Am. Chem. Soc.* **1975**, *97*, 6300−6305.
(29) Stenkamp, L. Z.; Davidson, E. R. *Theor. Chim. Acta* **1977**, *44*, 405−419.
(30) Nitzsche, L. E.; Davidson, E. R. *J. Chem. Phys.* **1978**, *68*, 3103−3109.
(31) Oliveros, E.; Riviere, M.; Teichteil, C.; Malrieu, P. *Chem. Phys. Lett.* **1978**, *57*, 220−223.
(32) Hirst, J. D.; Hirst, D. M.; Brooks, C. L., III. *J. Phys. Chem. A* **1997**, *101*, 4821−4827.
(33) Szalay, P. G.; Fogarasi, G. *Chem. Phys. Lett.* **1997**, *270*, 406−412.
(34) Serrano-Andrés, L.; Fülscher, M. P. *J. Am. Chem. Soc.* **1998**, *120*, 10912−10920.
(35) Pajcini, V.; Asher, S. A. *J. Am. Chem. Soc.* **1999**, *121*, 10942−10954.
(36) Bayliss, N. S.; McRae, E. G. *J. Phys. Chem.* **1954**, *58*, 1002−1006.
(37) Besley, N. A.; Hirst, J. D. *J. Phys. Chem. A* **1998**, *102*, 10791−10797.
(38) Taylor, P. R. *J. Am. Chem. Soc.* **1982**, *104*, 5248−5249.
(39) Del Bene, J. E. *J. Chem. Phys.* **1975**, *62*, 1961−1970.
(40) Sobolewski, A. L. *Photochem. Photobiol.* **1995**, *89*, 89−97.
(41) Kauss, M.; Webb, S. P. *J. Chem. Phys.* **1997**, *107*, 5771−5775.
(42) Besley, N. A.; Hirst, J. D. *J. Am. Chem. Soc.* **1999**, *121*, 8559−8566.
(43) Besley, N. A.; Hirst, J. D. *J. Mol. Struct., Theochem* **2000**, *506*, 161−167.

achieved. It is recognized generally that these models of solvent have a number of deficiencies.

Ideally, it is desirable to have a large number of explicitly defined water molecules. Once a large number of water molecules are considered it is also necessary to account for their numerous configurations. Car−Parrinello molecular dynamics[44] coupled with TDDFT provide a fully quantum mechanical description.[1,45] The use of a classical description of the solvent can reduce the cost of these calculations. This can be achieved through hybrid or sequential molecular mechanics/quantum mechanics (MM/QM) methodologies. In a hybrid scheme the classical and quantum mechanic regions are interfaced directly,[46−48] whereas in the sequential approach, a simulation of the liquid is used to generate structures that are then used in subsequent quantum mechanics calculations. In recent years, this approach has been pioneered by Canuto, Coutinho, and coworkers.[49−52] In their calculations, the structures of the solute and solvent are kept fixed while a large number of solvent configurations are selected from a Monte Carlo simulation using an autocorrelation function. Self-consistent field with intermediate neglect of differential overlap (INDO) followed by singly excited configuration interaction (CIS) calculations are used to determine excitation energies. Although unable to determine excitation energies accurately, this method can compute solvatochromic shifts. This, of course, relies on a systematic cancellation of errors between the transition energies for the isolated and solvated molecule. This methodology has been applied to formamide[51] and NMA[52] in aqueous solution. In these studies, a blue-shift of 0.20 eV for the nπ^* band and red-shift of 0.10 eV for the $\pi_{nb}\pi^*$ band were reported for formamide. Corresponding shifts of +0.22 and −0.15 eV for the nπ^* and $\pi_{nb}\pi^*$ bands of NMA were found.

In this article, we investigate the electronic spectra of a number of amides in gas phase and formamide in aqueous solution. First, gas-phase classical molecular dynamics (MD) simulations are used to generate configurations for use in subsequent TDDFT calculations. This approach is relatively inexpensive. Consequently, an electronic spectrum can be generated through averaging over several hundred configurations. A much smoother picture of the electronic spectrum can be obtained along with the spectral shifts induced by the increase in temperature. Furthermore, the structural origin of thermal broadening is studied. From this analysis it is possible to parametrize the nπ^* and $\pi_{nb}\pi^*$ transition energies based on structural features of the ground state. This allows electronic spectra arising from these transitions to be computed directly from the MD simulation without the need for additional quantum chemical calculations. Second, a sequential MM/QM approach is used to generate spectra in aqueous solution. In these calculations, a relatively large number of water molecules are included within the TDDFT calculations using a new approach that allows the calculation of excited states in solution at a reduced computational cost.[53] This approach can provide a quantitative determination of amide electronic spectra in solution.

Computational Details

Molecular Dynamics Simulations. All MD simulations were performed using the CHARMM program[54] with the CHARMM22 all-hydrogen parameters.[55] Simulations were performed at constant energy and volume, with a time step of 1 fs. The amide structure was not constrained in any fashion during the simulation. Simulations incorporating solvent used periodic boundary conditions with a box containing one solute molecule and 216 water molecules. The box was a cube of side 18.856 Å, giving a water density of 0.0334 molecules Å^{-3}. Intermolecular interactions were modeled by the Lennard-Jones and Coulombic potentials with water potentials based on the TIP3P model.[56] A nonbonded cutoff radius of 9 Å was used. The initial configurations were obtained by taking a pre-equilibrated box, overlaying the amide solute at the center of the box and deleting any (typically 5−10) overlapping water molecules. All simulations consisted of an initial heating period, in which the temperature was increased from 0 K to the simulation temperature. The total heating time was 6 ps. The system was then equilibrated for 12 ps. During this interval, the velocities were scaled to ensure the temperature remained in the window of ±5 K of the simulation temperature. For each amide, 10 independent 200-ps simulations were performed. Structures were sampled every 5 ps to give 40 structures for each run. This resulted in 400 structures for each amide that were used in subsequent ab initio calculations to determine the excitation energies.

Quantum Chemistry. Vertical excitation energies and oscillator strengths for the singlet states were determined using TDDFT with the B3LYP exchange-correlation functional[57] with the aug-cc-pVDZ basis set,[58,59] within the Q-Chem software package.[60] This provided an accurate description of the amide nπ^* and $\pi_{nb}\pi^*$ excitation energies. At this level of theory, calculation of the amide excited states in the presence of a large number of solvent molecules is very demanding computationally. We used a new approach that performed the TDDFT excited-state calculation within a subset of electronic excitations between orbitals associated with the solute.[53] This approach yielded significant computational savings, while introducing only a small error. It required the definition of cutoffs for the selection of the occupied and virtual orbitals.

The occupied orbitals were selected using their Mulliken populations.[61] If $\{\tilde{\lambda}\}$ was the subset of basis functions centered on the solute atoms, κ_i^{occ} could be defined such that

$$\kappa_i^{occ} = \sum_{\tilde{\lambda}} M_{\tilde{\lambda}i}$$

where $M_{\lambda i}$ is the contribution to the Mulliken population of orbital i from basis function λ. Thus, κ_i^{occ} provided a measure of the atoms on which an orbital i was localized. In this study, an orbital i was included

(44) Car, R.; Parrinello, M. *Phys. Rev. Lett.* **1985**, *55*, 2471−2474.
(45) Bernasconi, L.; Sprik, M.; Hutter, J. *J. Chem. Phys.* **2003**, *119*, 12417−12431.
(46) Gao, J. L.; Xia, X. F. *Science* **1992**, *258*, 631−635.
(47) Röhrig, U. F.; Frank, I.; Hutter, J.; Laio, A.; VandeVondele, J.; Rothlisberger, U. *ChemPhysChem* **2003**, *4*, 1177−1182.
(48) Sulpizi, M.; Carloni, P.; Hutter, J.; Rothlisberger, U. *Phys. Chem. Chem. Phys.* **2003**, *5*, 4798−4805.
(49) Coutinho, K.; Canuto, S. *J. Chem. Phys.* **2000**, *113*, 9132−9139.
(50) Coutinho, K.; Canuto, S.; Zerner, M. C. *J. Chem. Phys.* **2000**, *112*, 9874−9880.
(51) Rocha, R. R.; Martins, V. M.; Coutinho, K.; Canuto, S. *Theor. Chim. Acc.* **2002**, *108*, 31−37.
(52) Rocha, W. R.; De Almeida, K. J.; Coutinho, K.; Canuto, S. *Chem. Phys. Lett.* **2001**, *345*, 171−178.
(53) Besley, N. A. *Chem. Phys. Lett.* **2004**, *390*, 124−129.
(54) Brooks, B. R.; Bruccoleri, R. E.; Olafson, B. D.; States, D. J.; Swaminathan, S.; Karplus, M. *J. Comput. Chem.* **1983**, *4*, 187−217.
(55) MacKerell, A. D., Jr.; Bashford, D.; Bellott, M.; Dunbrack, R. L., Jr.; Evenseck, J. D.; Field, M. J.; Fischer, S.; Gao, J.; Guo, H.; Ha, S.; Joseph-McCarthy, D.; Kuchnir, L.; Kuczera, K.; Lau, F. T. K.; Mattos, C.; Michnick, S.; Ngo, T.; Nguyen, D. T.; Prodhom, B.; Reiher, W. E., III; Roux, B.; Schlenkrich, M.; Smith, J. C.; Stote, R.; Straub, J.; Watanabe, M.; Wiorkiewicz-Kuczera, J.; Yin, D.; Karplus, M. *J. Phys. Chem. B* **1998**, *102*, 3586−3616.
(56) Jorgensen, W. L.; Chandrasekhar, J.; Madura, J. D. *J. Chem. Phys.* **1983**, *79*, 926−935.
(57) Stephens, P. J.; Devlin, F. J.; Chabalowski, C. F.; Frisch, M. J. *J. Phys. Chem.* **1994**, *98*, 11623−11627.
(58) Dunning, T. H., Jr. *J. Chem. Phys.* **1989**, *90*, 1007−1023.
(59) Kendall, R. A.; Dunning, T. H., Jr.; Harrison, R. J. *J. Chem. Phys.* **1992**, *96*, 6796−6806.

if $\kappa_i^{occ} > 0.4$ au. An analogous parameter κ_a^{vir} based on molecular orbital coefficients was evaluated for the virtual orbitals.

$$\kappa_a^{vir} = \sum_{\tilde{\lambda}} |c_{\tilde{\lambda}a}|^2$$

In this work, a virtual orbital a was included if $\kappa_a^{vir} > 0.4$.

Since we were primarily interested in the electronic excitations of the amide solute, the more modest 6-31+G basis[62] set was used for the solvent molecules. Despite the computational savings gleaned from the method outlined, only a limited number of solvent molecules could be included, if averaging many configurations. Consequently, for each of the configurations taken from the MD simulation the water molecules were ordered with respect to their distance from the amide solute, which was defined as the distance from the center of the C−N bond to the oxygen atom of the water. Subsequently, the nearest 16 solvent molecules were retained explicitly within the QM calculation. Of the remaining solvent molecules, the nearest 24 were included as point charges. Charges of −0.820 au and +0.410 au, derived from a distributed multipole analysis[63] of gas-phase water using MOLPRO,[64] were used for oxygen and hydrogen, respectively. For each of the 400 configurations, vertical excitation energies of the lowest 40−50 states were computed to capture the spectra in the range 0−10 eV. This resulted in more than 16 000 electronic excitations. The calculated intensities of all the computed excitations were distributed into 0.01 eV energy divisions, and the spectra were plotted.

Results and Discussion

Gas Phase. Figure 2 shows the computed electronic spectra of gas-phase formamide at a range of temperatures. At low temperature, little broadening of the spectral lines occurs and distinct bands can be identified and assigned to nπ^*, $\pi_{nb}\pi^*$, and Rydberg transitions. As the temperature is increased, these bands broaden and merge. At 300 K only a few distinct bands occur. Bands at low energy arising from the n → 3s, π → 3s, and n → 3p Rydberg transitions remain. The broad $\pi_{nb}\pi^*$ band occurs with a maximum at approximately 7.6 eV, in good agreement with experiment. However, the results show that some of the intensity of this band arises from n → 3p and π_{nb} → 3p transitions. At higher energy, a number of distinct bands arising from n → 3d, π_{nb} → 3d, and n′ → 3s transitions are observed. These bands correspond to the Q-band. For formamide, there is no evidence of the $\pi_b\pi^*$ band in the spectral range 0−10 eV, consistent with previous work, which predicts this band to lie at 10.5 eV.[24]

The room temperature spectrum of formamide can be seen more clearly in Figure 3, which shows calculated spectra at 300 K for a variety of amides. The formamide spectrum shows evidence of sharp peaks superimposed on the intense $\pi_{nb}\pi^*$ band

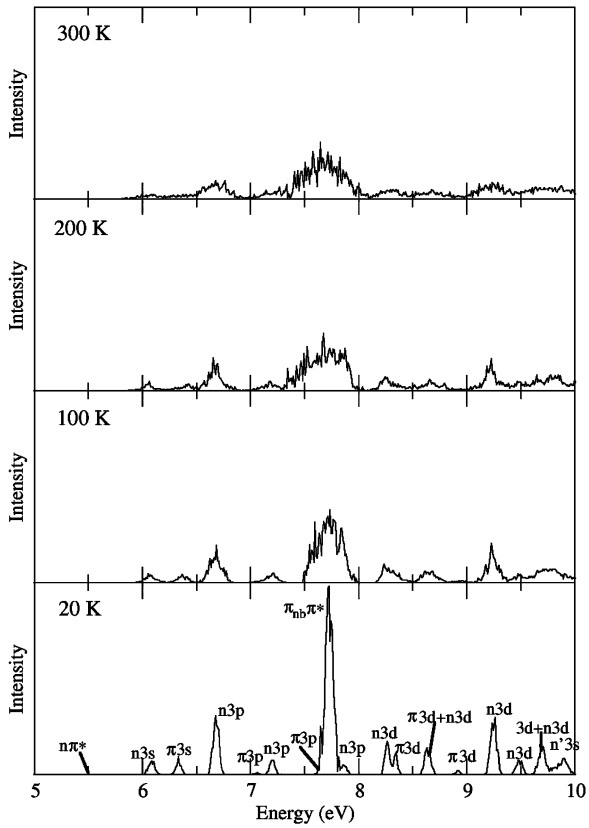

Figure 2. Electronic spectrum of gas-phase formamide at different temperatures.

and a distinct shoulder on the low energy side. These features are observed in reported experimental spectra.[21,23] The calculated formamide spectrum also shows a peak at ∼6.7 eV, which corresponds to a n → 3p Rydberg transition. In experiment, this peak merges with the $\pi_{nb}\pi^*$ band to form a broad shoulder. The two distinct peaks arise from a slight overestimation of the $\pi_{nb}\pi^*$ band in conjunction with an underestimation of the Rydberg transition energy. The calculation of excitation energies for transitions to Rydberg states has been discussed extensively in the literature.[65−67] The incorrect asymptotic form of exchange-correlation functionals leads to a significant errors in predicted excitation energies for Rydberg states. This problem can be addressed through the use of asymptotically corrected functions.[66] Excitation energies for formamide have been reported using the local density approximation with and without asymptotic correction.[26] These calculations showed a large (0.78 eV) underestimation of the n → 3p excitation energy without asymptotic correction. For the B3LYP functional, we would anticipate this underestimation to be smaller since B3LYP contains Hartree−Fock exchange, which does have the correct asymptotic behavior. However, some degree of underestimation of the n → 3p and other Rydberg excitation energies is expected. In addition, broadening will occur because of excitations to different vibrational states ("Franck−Condon" broadening), which may also result in the merging of the two peaks.

The gas-phase electronic spectrum of formamide presented here is similar to the previously reported spectrum computed

(60) Kong, J.; White, C. A.; Krylov, A. I.; Sherrill, C. D.; Adamson, R. D.; Furlani, T. R.; Lee, M. S.; Lee, A. M.; Gwaltney, S. R.; Adams, T. R.; Daschel, H.; Zhang, W.; Oschenfeld, C.; Gilbert, A. T. B.; Kedziora, G.; Maurice, D. R.; Nair, N.; Shao, Y.; Besley, N. A.; Maslen, P. E.; Dombroski, J. P.; Baker, J.; Byrd, E. F. C.; Voorhis, T. V.; Oumi, M.; Hirata, S.; Hsu, C. P.; Ishikawa, N.; Florian, J.; Warshel, A.; Johnson, G. B.; Gill, P. M. W.; Head-Gordon, M.; Pople, J. A. *J. Comput. Chem.* **2000**, *21*, 1532−1548.
(61) Mulliken, R. S. *J. Chem. Phys.* **1955**, *23*, 1833−1840.
(62) Hehre, W. J.; Ditchfield, R.; Pople, J. A. *J. Chem. Phys.* **1972**, *56*, 2257−2261.
(63) Stone, A. J. *Chem. Phys. Lett.* **1981**, *83*, 233−239.
(64) Amos, R. D.; Bernhardsson, A.; Berning, A.; Celani, P.; Cooper, D. L.; Deegan, M. J. O.; Dobbyn, A. J.; Eckart, F.; Hampel, C.; Hetzer, G.; Knowles, P. J.; Korona, T.; Lindh, R.; Lloyd, A. W.; McNicholas, S. J.; Manby, F. R.; Meyer, W.; Mura, M. E.; Nicklass, A.; Palmieri, P.; Pitzer, R.; Rauhut, G.; Schütz, M.; Schumann, U.; Stoll, H.; Stone, A. J.; Tarroni, R.; Thorsteinsson, T.; Werner, H.-J. *MOLPRO*, a package of ab initio programs designed by H.-J. Werner and P. J. Knowles, version 2002.1; University of Birmingham: Birmingham, U.K., 2002.
(65) Tozer, D. J.; Amos, R. D.; Handy, N. C.; Roos, B. O.; Serrano-Andrés, L. *Mol. Phys.* **1999**, *97*, 859−868.
(66) Tozer, D. J.; Handy, N. C. *J. Chem. Phys.* **1998**, *109*, 10180−10189.
(67) Tozer, D. J.; Handy, N. C. *Phys. Chem. Chem. Phys.* **2000**, *2*, 117−121.

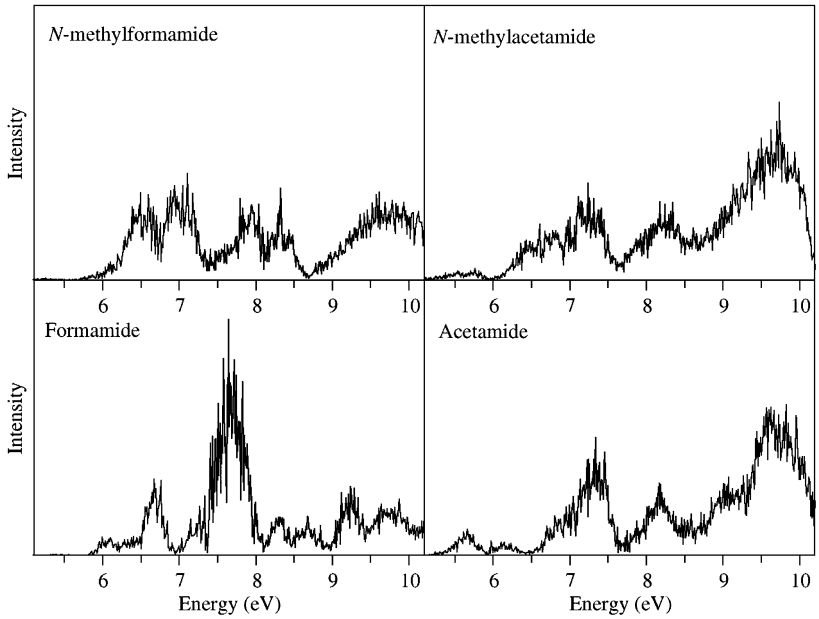

Figure 3. Computed electronic spectra of amides at 300 K.

using Car−Parinello MD coupled with TDDFT.[26] There is reasonable agreement between the predicted nπ^* and $\pi_{nb}\pi^*$ excitation energies. Furthermore, our calculations also indicate that the Q-band arises from n → 3d excitations. However, there is one significant difference in the nature of the R_1 band. Both studies show evidence of a band in approximately the correct region of the spectrum. When averaging over many structures, it is difficult to assign a band definitively to one transition. In the earlier study, the R_1 band was thought to arise from n → 3s and π_{nb} → 3s excitations, although an n3p state lies very close to the π_{nb}3s state. In this situation, the origin of nature of the band will depend on the relative intensities of the transitions. While the R_1 band in this study does contain contributions from n → 3s and π_{nb} → 3s excitations, the intensity does come predominantly from n → 3p excitations. However, if an asymptotically corrected functional was used, the balance of these contributions to the R_1 band may change.

The spectra of *N*-methylformamide (NMF), NMA, and acetamide have three dominant bands with the central band less intense than the other two. Also, the sharp Rydberg bands present for formamide are less prominent. The lower energy band arises from a superposition of the $\pi_{nb} \rightarrow \pi^*$, n → 3p, and π_{nb} → 3p transitions, the middle band from π_{nb} → 3d and n → 3d transitions, and the high energy band from $\pi_b \rightarrow \pi^*$ and Rydberg transitions. These spectra have a slightly different form than formamide. The $\pi_{nb}\pi^*$ bands are less dominant, and the $\pi_b\pi^*$ band can be identified. Since formamide is smaller than the other amides and does not contain relatively bulky methyl groups, the magnitude of the structural distortion may be expected to be less, and therefore less broadening of the spectral bands would be anticipated. This is reflected by the smaller number of distinct bands that can be identified in the spectra of the larger amides, particularly for NMA and acetamide. Less experimental data are available for acetamide, NMF, and NMA. The gas-phase electronic spectrum of *N*,*N*-dimethylacetamide has been reported[21] and is qualitatively similar to those presented here. There is a good agreement with the available experimental data. The predicted $\pi_{nb}\pi^*$ excitation energies are 7.66, 7.20, 6.88, and 6.86 eV for formamide, acetamide, NMF, and NMA, respectively. These compare with 7.4, 7.4, 7.0, and 6.8 eV from experiment.[19,21,23]

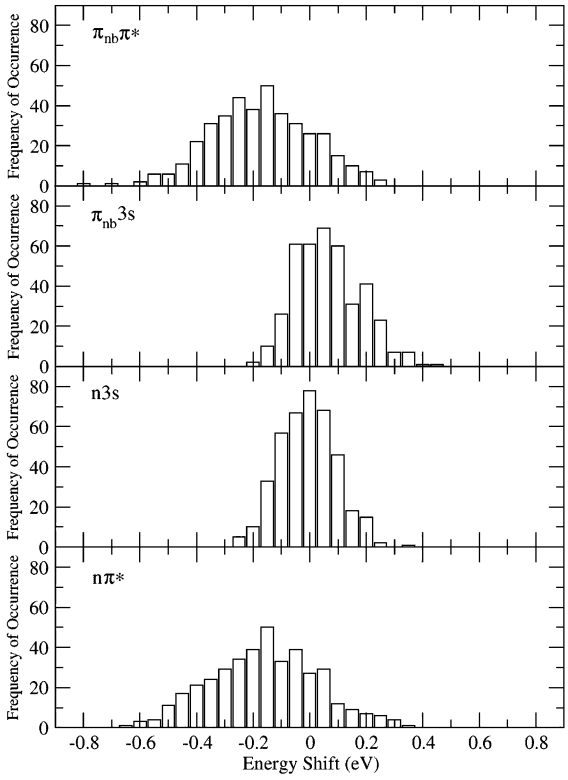

Figure 4. Distribution of shifts in the formamide excitation energies between 0 and 300 K simulations.

Figure 4 shows histograms depicting the shifts in excitation energies at 300 K relative to 0 K for low-lying Rydberg and valence states of formamide. Excitation energies at 0 K were calculated at the B3LYP/aug-cc-pVDZ minimum energy structure. For the Rydberg states, the distribution is relatively narrow and symmetric about 0 eV. For the valence nπ^* and $\pi_{nb}\pi^*$ states, the distributions are broader, and there is a distinct asym-

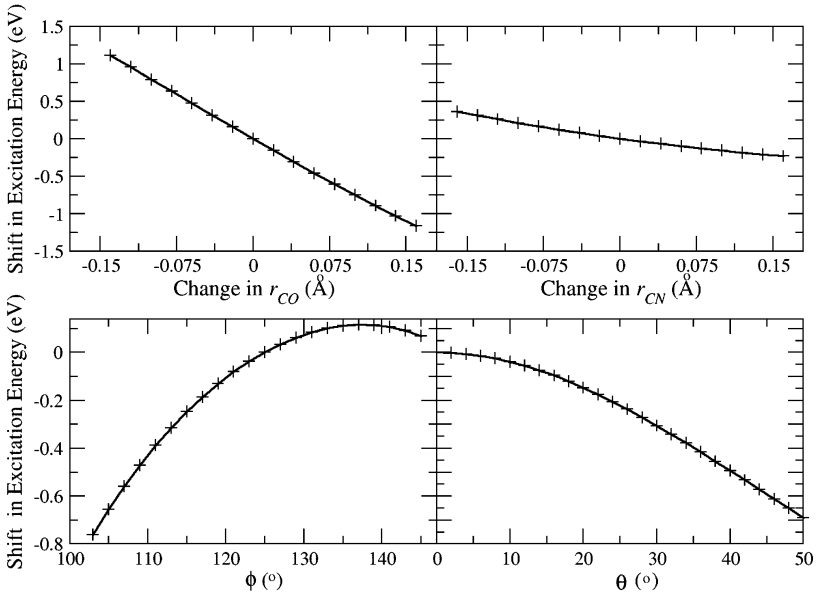

Figure 5. Variation of formamide nπ^* excitation energy with structural parameters.

Table 1. Electronic Transition Energies in Electronvolts and Oscillator Strengths in Parentheses

	formamide		acetamide		NMF		NMA	
state	300 K	0 K	300 K	0 K	300 K	0 K	300 K	0 K
nπ^*	5.36 (0.00)	5.52 (0.00)	5.34 (0.00)	5.48 (0.00)	5.21 (0.00)	5.50 (0.00)	5.27 (0.01)	5.61 (0.00)
n3s	6.07 (0.02)	6.08 (0.02)	5.65 (0.02)	5.71 (0.03)	6.05 (0.01)	6.10 (0.00)	5.74 (0.01)	5.71 (0.01)
π3s	6.39 (0.02)	6.33 (0.02)	6.12 (0.01)	6.10 (0.01)	5.84 (0.00)	5.97 (0.00)	5.57 (0.00)	5.64 (0.00)
$\pi_{nb}\pi^*$	7.66 (0.23)	7.83 (0.30)	7.20 (0.08)	7.35 (0.07)	6.88 (0.10)	7.25 (0.15)	6.86 (0.05)	7.11 (0.10)

metry indicating that red-shifted excitation energies are more likely. This is quantified in Table 1. For the Rydberg states, there is little difference between the average excitation energies and oscillator strengths at 300 and 0 K. However, for the nπ^* and $\pi_{nb}\pi^*$ states of all the amides, there is a reduction in the excitation energy of approximately 0.1−0.35 eV. This red-shift is larger for NMF and NMA. Shifts of this magnitude are likely to be present for all electronic transitions in which there is a large difference between the minimum ground- and excited-states structures. There is also a loss of intensity for the $\pi_{nb}\pi^*$ band.

In the ground state of amides, the heavy atoms have been shown to lie in a plane.[24,33] Houk and co-workers have reported optimized structures for amide nπ^* and $\pi_{nb}\pi^*$ excited states.[68] In addition to a lengthening of the C═O (r_{CO}) and C−N (r_{CN}) bonds, these structures show a large twist in the amide group. This can be readily rationalized by considering the n, π_{nb}, and π^* orbitals (Figure 1). Lengthening of the C═O and C−N bonds and twisting of the C−N bond relative to the C═O bond are likely to stabilize the π^* orbital since antibonding regions of the orbital will be moved further apart. The effect on the π_{nb} and n orbitals should be smaller. Thus, structural distortions of this nature will stabilize the excited state relative to the ground state and lead to a red-shift in the excitation energy. Following similar arguments, a shortening of the C═O and C−N bond lengths would lead to a blue-shift in the nπ^* and $\pi_{nb}\pi^*$ excitation energies. A dependence of the nπ^* excitation energy with C═O bond length has been reported for acetone.[69,70] The excited-state structures also exhibit a decrease in the NCO bond angle. Figure 5 shows the variation in the nπ^* excitation energy of formamide with the four coordinates r_{CO}, r_{CN}, θ (the OCNH dihedral angle, <180°), and ϕ (the NCO bond angle). For all the coordinates there is a smooth variation of the excitation energy. The excitation energy is most sensitive to changes in r_{CO}; previous work[68] has shown the π^* orbital to lie predominantly on the carbon and oxygen atoms.

If these four coordinates are critical in inducing a shift in the transition energies, then for a given structure the excitation energies can be predicted. In this work we have assumed an independent model. The shifts in the excitation energies as a function of the coordinates are individually fitted by cubic splines, and the total shift is determined in an additive fashion. This approach has the advantage that much less data are required to provide a good fit than if the shifts induced by the different coordinates are treated as coupled. Fits in which the coordinates are paired provided only a minor improvement. For the nπ^* transition, the shift in electronvolts (relative to 5.5884 eV) is given by:

$$16.3386 - 7.8128x + 2.0557x^2 + 8.8467x^3 - 1.8365y + 2.6210y^2 - 0.8767y^3 + 0.0005\theta - 0.0005\theta^2 + 3.4660 \times 10^{-6}\theta^3 + 0.2643\phi - 0.0012\phi^2 + 1.3160\phi^3 \quad (1)$$

where x is the C═O bond length (r_{CO}), y is the C−N bond length

(68) Li, Y.; Garrell, R. L.; Houk, K. N. *J. Am. Chem. Soc.* **1991**, *113*, 5895−5896.

(69) Blair, J. T.; Krogh-Jespersen, K.; Levy, R. M. *J. Am. Chem. Soc.* **1989**, *111*, 6948−6956.

(70) Coutinho, K.; Saavedra, N.; Canuto, S. *J. Mol. Struct., Theochem* **1999**, *466*, 69−75.

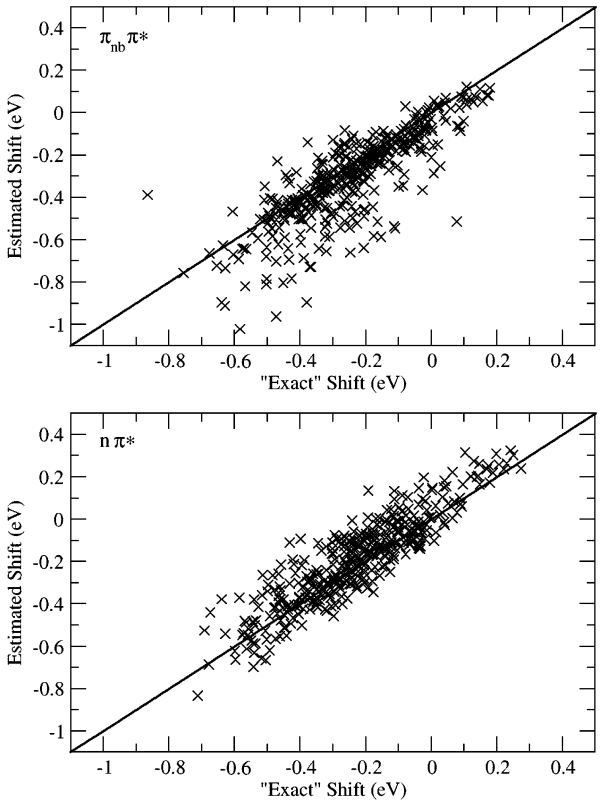

Figure 6. Accuracy of the estimated shifts for formamide nπ^* and $\pi_{nb}\pi^*$ transitions.

(r_{CN}), θ is the OCNH dihedral angle (in degrees and less than 180°), and ϕ is the NCO bond angle (in degrees). For the $\pi_{nb}\pi^*$ transition, the shift in electronvolts (relative to 7.9040 eV) is given by:

$$-2.9195 - 4.1018x - 6.7624x^2 + 2.9532x^3 - 2.2796y - 19.9604y^2 + 56.6489y^3 + 0.0113\theta - 0.0016\theta^2 + 0.00002\theta^3 - 0.0768\phi + 0.0016\phi^2 - 6.0165 \times 10^{-6}\phi^3 \quad (2)$$

and for short C−N bond lengths ($y < -0.095$):

$$-2.6238 - 4.1018x - 6.7624x^2 + 2.9532x^3 + 1.4653y + 0.0113\theta - 0.0016\theta^2 + 0.00002\theta^3 - 0.0768\phi + 0.0016\phi^2 - 6.0165 \times 10^{-6}\phi^3 \quad (3)$$

Figure 6 shows the agreement between the predicted excitation energies from this model and the excitation energies from the TDDFT calculations. The agreement for the nπ^* state is good ($R^2 = 0.80$, $n = 400$) and a little lower for the $\pi_{nb}\pi^*$ state ($R^2 = 0.67$, $n = 400$). It is more difficult to model the $\pi_{nb}\pi^*$ transition, since it tends to be mixed with Rydberg excitations. However, for both transitions the agreement is sufficiently good to calculate spectra. Figure 7 shows the results of these calculations for formamide nπ^* and $\pi_{nb}\pi^*$ bands, where spectra are constructed from 40 000 structures drawn from ten 4000 ps simulations and the average oscillator strengths (Table 1) are assumed for all transitions. The variation of the structure throughout the simulation is summarized in Table 2. For both states, relatively smooth band profiles are obtained. For the $\pi_{nb}\pi^*$ state, the spectrum illustrates that much of the intensity arises from Rydberg transitions, particularly on the high energy side. This approach of computing excitation energies through a parametrization based on ground-state geometrical features may be extended and used to compute electronic spectra of much larger systems, such as proteins, where direct quantum chemical calculations are not possible.

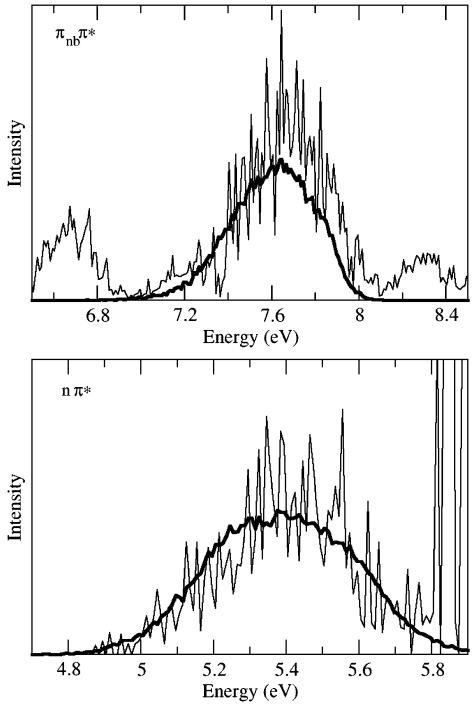

Figure 7. Computed formamide nπ^* and $\pi_{nb}\pi^*$ band profiles from TDDFT (narrow line) and estimated from structure (bold line).

Table 2. Variation of Structural Parameters for Formamide during the Simulations

	r_{CO}/Å	r_{CN}/Å	θ/deg	ϕ/deg
optimized structure	1.22	1.36	0.00	124.9
	Gas Phase			
mean	1.23	1.35	9.2	121.8
maximum	1.28	1.42	38.6	131.8
minimum	1.16	1.28	0.0	111.3
standard deviation	0.02	0.03	7.1	3.5
	In Solution			
mean	1.23	1.35	10.9	121.7
maximum	1.31	1.42	45.7	129.1
minimum	1.17	1.28	0.1	112.8
standard deviation	0.02	0.02	8.2	2.7

Formamide in Aqueous Solution. Figure 8 shows the average mean absolute error introduced by the truncation of the single excitation space as the number of solvent molecules is increased. Each point represents an average of five configurations drawn randomly from the MD simulations, with an error bar representing the standard deviation. The variation in the error shows no obvious trend, and on average an error of ~0.05 eV can be expected with no systematic over- or underestimation. However, in addition to the computational savings, there are other benefits to the truncated scheme. With full TDDFT, as the number of solvent molecules increases the $\pi_{nb}\pi^*$ band becomes mixed among a large number of solvent transitions. This makes the $\pi_{nb}\pi^*$ band very difficult to identify. This is much less of a problem within the truncated scheme, where the $\pi_{nb}\pi^*$ band can usually be assigned reliably.

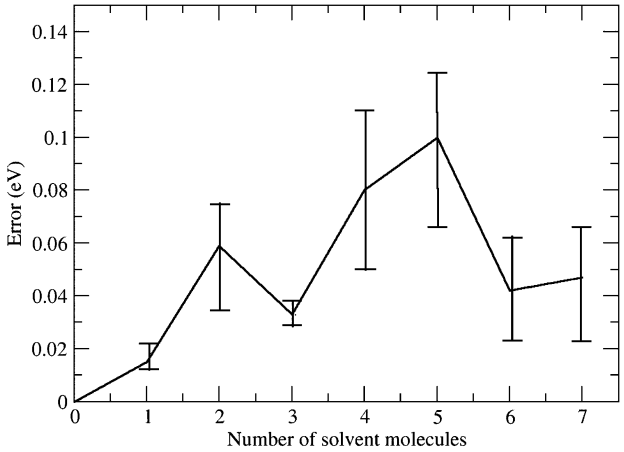

Figure 8. Average error introduced through truncating the single excitation space.

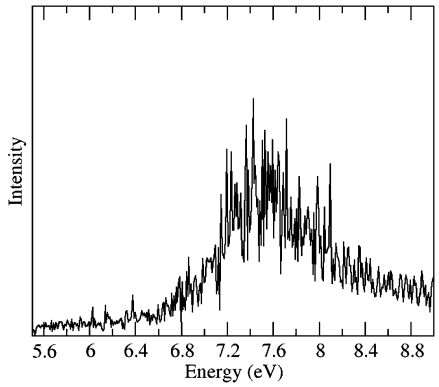

Figure 9. Computed electronic spectrum of formamide in aqueous solution.

The computed electronic spectrum of formamide in water is shown in Figure 9. The general form of the spectrum matches experiment,[21] with a broad band that is red-shifted compared to gas phase. The spectrum is not smooth, and this reflects that averaging 400 configurations is too little to achieve convergence. At low energy (5.5−6.8 eV), there is a constant low level of intensity. This intensity arises from nπ^*, Rydberg, and solute → solvent charge-transfer transitions. The appearance of Rydberg and charge-transfer transitions in this region of the spectrum is initially surprising and may be physical or due to deficiencies in the TDDFT. It is expected that the Rydberg bands would not be observed in the condensed-phase spectrum.[21,37] This is due to destabilization of the Rydberg states by the solvent molecules. In the present calculations, the transition energies of the Rydberg states do increase. This is illustrated by the absence of the prominent Rydberg band at ∼6.7 eV in the gas-phase spectrum. For nonasymptotically corrected exchange correlation functionals, the Rydberg states are predicted to lie too low, and thus the destabilization observed is insufficient to raise their energy above the $\pi_{nb}\pi^*$ state. In analogous single excitation configuration interaction calculations, for the majority of configurations the two lowest states are nπ^* and $\pi_{nb}\pi^*$. It has also been shown that TDDFT does not describe well the movement of electrons over large distances. This is significant for charge-transfer transitions.[65] In a recent study of acetone in aqueous solution,[45] this led to the observation of spurious solvent → solute and solvent → solvent charge-transfer bands. In this work, solvent → solute and solvent → solvent charge-transfer transitions do not occur because of the truncation of the occupied space. However, because of the more diffuse nature of the virtual orbitals, identifying the solute virtual orbitals is more problematic, and a number of solvent virtual orbitals will be included in the truncated virtual space. This results in the appearance of solute → solvent charge-transfer bands. For these reasons, we will focus our discussion on the properties of the valence states.

The mean value for the $\pi_{nb}\pi^*$ excitation energy is 7.43 eV. Compared to the gas-phase value at 0 K, this represents a red-shift of −0.40 eV. However, it is important to use the appropriate gas-phase value at 300 K, resulting in a red-shift of −0.23 eV. This is smaller than the observed experimental value, although larger than the red-shift found using a similar approach with the excitation energies determined using more approximate methods.[51] This underestimation could have a number of sources. An adequate description of the amide excited states required the extensive aug-cc-pVDZ basis set, and thus only the first solvation shell of solvent could be included. While this represents a relatively large number of water molecules, it will not fully capture the long-range effects on the solvent.

The Mulliken populations[61] of the oxygen atoms of the water molecules can provide a rough estimate of the degree to which their electron distributions are polarized. In a complex containing formamide and five water molecules, the average solvent oxygen Mulliken population is −0.91 au. The average value for the same water molecules is −0.94 and −1.03 au in calculations with 10 and 16 water molecules, respectively. This shows that, as the number of water molecules increases, the environment immediately around the solute becomes more polar. Thus, even if the solute does not feel the effect of the second and third shells of solvent directly, they can have an indirect effect through increased polarization of the neighboring solvent molecules. The inclusion of second solvation shell as point charges should capture this effect. The addition of point charges leads to a value of −1.06 au. However, this probably does not account fully for the additional solvent molecules. In the work of Rocha et al.,[51] the first solvation shell captured approximately 70% of the total shift in the $\pi_{nb}\pi^*$ excitation energy. Consequently, the limiting solvatochromic shift within the current calculations would be anticipated to be in the region of −0.33 eV.

A further reason for the observed underestimation of the red-shift of the $\pi_{nb}\pi^*$ band is the modeling of the fast response of the solvent.[71,72] Upon electronic excitation, the solute will no longer be in equilibrium with the solvent. The response of the solvent can be partitioned into two components.[73] The slow or inertial component consists of the solvent nuclear motions; these are assumed to be constant. However, the electronic polarization of the solvent changes on a fast time scale. This is the so-called fast or noninertial response of the solvent. If there is a large change in dipole moment, this effect can be significant. Physically, if the dipole moment increases, then the polarization of the solvent will increase, which in turn leads to a greater stabilizing interaction. The contribution of the fast response to solvatochromic shifts can be determined within reaction field

(71) Cramer, C. J.; Truhlar, D. G. *Chem. Rev.* **1999**, *99*, 2161−2200.
(72) Li, J.; Cramer, C. J.; Truhlar, D. G. *Int. J. Quantum Chem.* **2000**, *77*, 264−280.
(73) Bonaccorsi, R.; Cimiraglia, R.; Tomasi, J. *J. Comput. Chem.* **1983**, *4*, 567−577.

theories and has been discussed in detail.[71,72,74] Li et al.[72] have evaluated the contribution of different components to the solvatochromic shifts for the nπ^* excitation of acetone in different solvents.

We have used CASSCF/SCRF calculations to estimate the contribution of the fast response of the solvent to the solvatochromic shift. CASSCF/SCRF calculations were performed for the nπ^* and $\pi_{nb}\pi^*$ states of formamide. The solute is placed in a spherical cavity of radius 6.0 a_0, embedded in a dielectric continuum characterized by a dielectric constant of 80.0 and optical refractive index of 1.33. Generally, contracted atomic natural orbital basis sets were used with the following contractions: C, N, O 4s3p1d, and H 2s. These calculations reproduce the observed red-shift in the $\pi_{nb}\pi^*$ state. Further details of these calculations can be found elsewhere.[37] The contribution of the fast response to the red-shift is estimated to be 0.07−0.10 eV for the $\pi_{nb}\pi^*$ state and ∼0.02 eV for the nπ^* state. This is consistent with qualitative arguments based on the dipole moments of the states. There is little difference between the dipole moments of the ground and nπ^* states. However, there is a large increase for the $\pi_{nb}\pi^*$ state. Accounting for this correction brings our estimate of the red-shift into much closer agreement with experiment. However, the *change* in this adjustment between different solvent configurations is likely to be small, and thus the shape of the band profile will not change.

The average transition energy for the nπ^* transition is 5.88 eV, representing a shift of +0.52 eV. The lack of reliable experimental data makes direct comparison with experiment difficult. The magnitude of this shift is slightly smaller than those found in a previous study of small formamide−water clusters,[42] which is consistent with the finding that small cluster calculations can lead to an overestimation of the effects arising from hydrogen bonds.[70]

A number of factors can give rise to a solvatochromic shift. These can be due to a difference in the strength of interaction between the solvent and the ground and excited state of the solute. However, a shift can arise because of structural changes on the ground state induced by the solvent. This has been discussed for the nπ^* transition in acetone,[70] where it was noted that the structural contribution to the solvatochroism was in opposition (red-shift) to the overall blue-shift that is observed. The variation of the structural parameters in solution (Table 2) shows a small increase in r_{CN} and θ. Both of these effects should lead to a red-shift contribution to the solvatochroism for both nπ^* and $\pi_{nb}\pi^*$ transitions. This can be quantified. Analysis of formamide structures drawn from the condensed-phase simulations shows red-shifts of 0.07 and 0.05 eV for the nπ^* and $\pi_{nb}\pi^*$ states, respectively. For the nπ^* transition, this shift due to structural changes is overwhelmed by a much larger blue-shift, most likely arising from the difference in the hydrogen bonds strengths between the ground and excited states. For the $\pi_{nb}\pi^*$ state, this red-shift is increased because of the shift induced by electrostatics.

Conclusions

The vast majority of theoretical calculations of electronic spectra are appropriate for the system at 0 K. In such calculations, electronic transitions are represented by a single excitation and associated oscillator strength. However, in experimental spectra measured at higher temperatures, electronic transitions are represented by bands with a distinct shape. Much of this broadening of the spectral bands is thermal in origin. In this study, a combination of classical MD simulations and TDDFT has been used to study the electronic spectra of amides in gas phase and solution at 300 K. This combination provides spectra that capture important spectral features observed in experiment. For the low-lying Rydberg states, the thermal broadening of the bands shows no large bias toward a blue- or red-shift and the computed average excitation energies are close to those for the global minima structures. However, for the valence nπ^* and $\pi_{nb}\pi^*$ states, a significant red-shift is observed, indicating that effects due to temperature can be significant. The origin of these shifts can be rationalized on the basis of the electronic structure of formamide. A model has been constructed in which the nπ^* and $\pi_{nb}\pi^*$ excitation energies can be predicted from structure of the ground state. Consequently, spectra for the valence states can be generated directly from the MD simulation, without the need for additional quantum chemical calculations. This approach has an extremely low computational cost and allows the generation of spectra from a very large number of structures, which is required to achieve converged band profiles. Such an approach may provide a route to the calculation of electronic spectra of much larger systems such as proteins, where direct quantum mechanical calculations are not feasible.

The study of molecular properties in the condensed phase is most often achieved using simple solvent models, such as a continuum or a small number of explicit solvent molecules. Recently, there has been progress toward more sophisticated descriptions of the solvent. The simulation of electronic spectra in solution with solvent models containing many solvent molecules is a very demanding problem. One approach is ab initio molecular dynamics, which has a number of advantages, but is impractical for studying large systems or long simulation periods. As a result, there is a need for less computationally demanding methods that maintain a quantitative level of accuracy. In this work, we have used one such approach to study the electronic spectrum of formamide using a solvent model that contains a much larger number of explicit solvent molecules employing correlated quantum chemical methods. This requires a new approach that reduces the cost of this type of calculation through restricting excitations to those between orbitals associated with the solute. This allows the direct computation of spectra, as opposed to the computation of solvatochromic shifts, which is possible with extensive solvent models using cheaper, more approximate methods. The spectra obtained do generally reproduce experimentally the band profile observed in experiment. However, the obtained red-shift in the $\pi_{nb}\pi^*$ band is smaller. If convergence with respect to the number of solvent molecules and the instantaneous response of the solvent polarization are considered, a shift much closer to experiment is obtained. The structural changes in formamide induced by the solvent cause a small red-shift of 0.07 and 0.05 eV in the nπ^* and $\pi_{nb}\pi^*$ bands, respectively. For the nπ^* band, this is offset by a much larger blue-shift, probably due to differences in the strength of hydrogen bonds between the ground and excited states. For the $\pi_{nb}\pi^*$ band, electrostatic interactions lead to an increase in this red-shift.

(74) Serrano-Andres, L.; Fulscher, M. P.; Karlstrom, G. *Int. J. Quantum Chem.* **1997**, *65*, 167−181.

The study of spectroscopic properties of species in condensed phases through fully atomistic simulation provides new insight into many chemical and biological processes. This study presents a framework that can be readily extended to larger systems of interest. We are currently extending the methodology to the study of polypeptides.

Acknowledgment. This work was supported through the Engineering and Physical Sciences Research Council through the award of an Advanced Research Fellowship (GR/R77636) to N.A.B., GR/N66971, and a Joint Research Equipment Initiative Grant (GR/R62052).

JA047603L